ELSEVIER

Journal of Photochemistry and Photobiology A: Chemistry 154 (2003) 245–257

Journal of Photochemistry and Photobiology A:Chemistry

www.elsevier.com/locate/jphotochem

Photophysical and photochemical properties of amitriptyline and nortriptyline hydrochloride: a 266 nm nanosecond laser flash and theoretical study

Rafael Arce [a,*], Carmelo García [b,1], Rolando Oyola [a], Luis Piñero [b], Ileana Nieves [b], Nadya Cruz [b]

[a] *Department of Chemistry, University of Puerto Rico, Río Piedras Campus, P.O. Box 23346, San Juan 00931-3346, Puerto Rico*
[b] *Department of Chemistry, University of Puerto Rico, Humacao Campus, Humacao 00791-4300, Puerto Rico*

Received 19 July 2002; received in revised form 19 September 2002; accepted 19 September 2002

Abstract

Amitriptyline (AMI) and nortriptyline (NT) hydrochlorides were studied by 266 nm laser transient absorption spectroscopy and quantum theoretical calculations. Both drugs photoionize through a biphotonic mechanism producing a radical cation and the solvated electron. A triplet excited state in a twisted conformation around the exocyclic bond is proposed as the intermediate state in the photoionization process. The solvated electron reacts with the ground state drug molecules with rate constants of 6.5 and 5.5×10^9 M^{-1} s^{-1} to form electron adducts, that absorb in the same wavelength region as the radical cation. Photosensitization experiments using thioxanthone triplet state as the sensitizer demonstrated that AMI or NT quenches this state by a mechanism that depends on the protonation of the amino group in the alkylamine side chain. The protonated species favors energy transfer, while the unprotonated species produces the tricyclic antidepressive radical cation of these drugs and the thioxanthone ketyl radical. These results follow the Rehm–Weller equation for an electron transfer mechanism. Quantum theoretical calculations indicate that ground and excited singlet states photophysical properties of these molecules are determined by the 1,2-diphenylethane system with little participation of the exocyclic double bond. The presence of these primary radicals could explain the reported Type I photodamaging effects for these drugs.

Keywords: Amitriptyline; Nortriptyline; Laser flash photolysis; Tricyclic antidepressive; Photochemistry and quantum theoretical calculations

1. Introduction

Amitriptyline (AMI) and nortriptyline (NT) (Fig. 1) are tricyclics antidepressant drugs (TCA) with a dibenzocycloheptene fused ring widely used in mental health care [1–3]. They lack the sulfur and nitrogen atoms found in the promazine derivatives. A "surfactant-like" behavior is conferred by the presence of the alkyl amine side chain. Model studies for the interaction of several TCA with dodecyldimethylammonium chloride [4] and sodium dodecyl sulfate micelles [5] have shown that AMI adopts an extended conformation in the micelle. The *N*-methyl propylamine side chain resides close to the micelle surface and the tricyclic group penetrates the hydrophobic region. These results indicate that the interaction of TCAs with biological membranes is fundamental in their biological activity. A demethylation process converts AMI into NT, one of its main metabolic products [6,7]. Since both molecules have similar molecular structures, their chemical properties are not expected to differ much. As a matter of fact, patients treated with these TCAs show similar side effects when exposed to sunlight, although to different extent when compared to other related TCAs [8,9]. The major side effect induced by these two TCAs is a skin slate-gray discoloration, which can last for years after cessation of therapy [10].

Recently, Dall'Acqua et al. [11] reported that AMI phototoxicity can promote cell death even at a concentration of 100 μM and UVA doses in the range of 3.3–6.6 J cm^{-2}. A negligible production of singlet oxygen (Type II photo-

Abbreviations: AMI, amitriptyline-free base; AMI-HCl, amitriptyline hydrochloride; DPE, 1,1-diphenylethylene; 1,2-DPE, 1,2-diphenylethane; NT, nortriptyline-free base; NT-HCl, nortriptyline hydrochloride; PBS 7.4, pH = 7.4 phosphate buffer saline; PTL-HCl, protriptyline hydrochloride; PTL, protriptyline-free base; TBAP, ter-butyl ammonium perchlorate; TCA, tricyclic antidepressants; TX, thioxanthone

* Corresponding author. Tel.: +787-764-0000x2433; fax: +787-759-6885.
E-mail addresses: rarce@goliath.cnnet.clu.edu (R. Arce), c_garcia@cuhac.upr.clu.edu (C. García).
[1] Co-corresponding author. Tel.: +787-850-9387; fax: +787-850-9422.

1010-6030/03/$ – see front matter © 2003 Elsevier Science B.V. All rights reserved.
PII: S1010-6030(02)00353-2

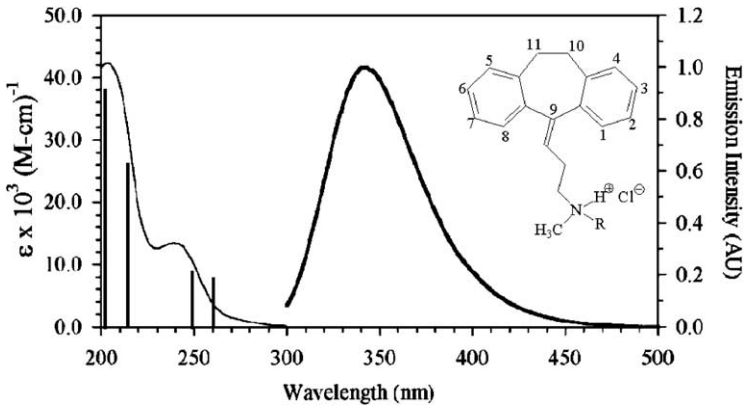

Fig. 1. Absorption and emission spectra of NT-HCl in acetonitrile; left: molar ground state absorption spectrum with vertical lines indicating the PM3 oscillator strengths, and right: emission spectrum (λ_{max} = 280 nm, Abs = 0.20). Inset: molecular structure of AMI-HCl (R = CH_3) and NT-HCl (R = H).

chemistry) was observed for AMI, whereas a significant production of superoxide anion (Type I photochemistry) was noted. Also, the drug photosensitized the peroxidation of linoleic acid. These results clearly demonstrated that a triplet state was not participating in those reactions. If Type II photochemistry is excluded as the responsible mechanism, then radicals intermediates should be involved in the photodamaging effects of these drugs. The steady-state photolysis of AMI and NT yields several photoproducts resulting from photofragmentation [12]. The proposed mechanism involves an electron and a proton transfer similar to that previously proposed for the photoreduction of amines [13].

However, the spectral properties of the AMI-HCl or NT-HCl participating in the photochemical processes were not reported. In this work, we present the characterization of AMI-HCl and NT-HCl primary transient intermediates generated by 266 nm nanosecond laser flash photolysis. The ground and excited singlet state properties of both drugs were measured in acetonitrile, methanol and PBS. Also, electrochemical oxidation potentials were determined for both molecules. Finally, quantum chemical calculations were performed to better explain their molecular properties such as ground state conformations, UV-Vis transitions and ionization.

2. Experimental

2.1. Materials

Amitriptyline hydrochloride (AMI-HCl), nortriptyline hydrochloride (NT-HCl) and thioxanthone (TX) were purchased from Sigma and used as received. The TCA-free base was obtained by sodium hydroxide addition to an aqueous solution of the corresponding hydrochloride, followed by ether extraction. Organic solvents and other reagents were high quality grade from well-known suppliers and used without further purification. Nitrogen and nitrous oxide were purchased from Air Products (Humacao, PR). Aqueous solutions were prepared with nanopure water.

2.2. Absorption and emission spectroscopy

Absorption spectra were taken with a HP 8453 UV-Vis photodiode array spectrophotometer. Luminescence was measured with a Spex Fluorolog Tau 3.11 spectrofluorometer (Spex Industries, NJ). The fluorescence quantum yield (ϕ_f) was calculated relative to tryptophan ($\phi_f = 0.13$) [14] according to the method of Demas and Crosby [15]. The excitation wavelength was set to 280 nm and the monochromator slits were set to 2.5 nm; reference and samples were optically matched ($A < 0.1$) and corrections were made for differences in the instrument sensitivity as a function of wavelength and for differences in refractive index. The fluorescence lifetime was measured using the frequency domain technique. Briefly, the AMI-HCl emission frequency response was measured against 1,4-bis[5-phenyl-2-oxazolyl]benzene (POPOP) in ethanol ($\tau_f = 1.35$ ns) using 280 nm excitation and the fluorescence was measured through a 300 nm long pass filter.

2.3. Nanosecond laser flash spectroscopy

The 266 nm nanosecond laser flash photolysis of the TCAs was used for the direct excitation and generation of their transient intermediates. Photosensitization studies using thioxanthone (TX) as triplet energy donor were performed using the 355 nm laser harmonic. Experiments were carried out using the corresponding harmonic output of a Nd/YAG laser Surelite II (Continuum, Santa Clara, CA) as the excitation source. All transient species were monitored at right angles to the laser beam using a 300 W Xenon arc lamp (Oriel Corp., Connecticut, USA). The probe beam was discriminated with a monochromator Model 305 (Acton Research, Massachusetts, USA) and detected with a Hamamatsu R928 five stage dynode wired photomultiplier

tube. The output from the photomultiplier was digitized with either a 400 MHz bandwidth oscilloscope Model 9310 (LeCroy Corp., New York, USA) or a Tektronix 3032B oscilloscope (Tektronix Corp., USA) for transients with lifetimes shorter than 200 ns. A flow system was used to ensure a fresh sample for each laser pulse. The whole spectrokinetic system was controlled with a custom software developed under LabView 5.1 (National Instruments, Austin, TX). The analysis of the decay curves were carried out using Levenberg–Marquardt non-linear fitting subroutines under LabView 5.1.

2.4. Electrochemical measurements

Electrochemical experiments were performed with a voltammetric analyzer BAS Model CV-50W. Solutions of protonated or unprotonated AMI or NT (1.0 mM) in acetonitrile or methanol, containing 0.1 M ter-butyl ammonium perchlorate (TBAP) as supporting electrolyte, were degassed with nitrogen before use. The measurements were carried out using glassy carbon as working electrode, a platinum wire as counter electrode and Ag/AgCl (sat.) ($E^0 = +0.222$ V) as reference electrode. Oxidation potentials in aqueous solutions were not measured due to the potential range limitations for this solvent ($-1.5 \leq V \leq 1.5$).

2.5. PM3/CI theoretical calculations

Geometry optimization using a combination of molecular mechanics (MM+), molecular dynamics and quantum mechanical calculations for closed shells (PM3/RHF/CI) and open shells (PM3/UHF) were performed with HyperChem 7.01 (HyperCube Inc., Florida) running on an SGI-320 with dual 450 MHz processors (Silicon Graphics, California). The MM+ method was used to pre-optimize all closed shell systems. At the semiempirical level, the optimizations were done with the Polak–Ribiere conjugated gradient protocol (1×10^{-5} convergence limit, 0.001 kcal (Å mol)$^{-1}$ RMS limit). The lowest energy conformations were found by randomly varying the chain's dihedral angle. To assure that the counter ion remains at the standard distance in the AMI-HCl and NT-HCl systems, the $H^+ \cdots Cl^-$ separation was restrained to 1.32 Å with a default force constant of 7 kcal mol^{-1} Å^{-2}. The optimization of the S_1 state was done with the half-electron method strategy with the S_1-Franck–Condon conformation. All molecular parameters were obtained with PM3/RHF/CI-single point calculations starting with the most stable PM3-optimized conformation and using three occupied and three virtual orbitals. The gas phase ionization potential (IP_g) was taken either as the negative of the HOMO energy (Koopman's theorem) or calculated from the formation enthalpies of the molecule and the corresponding cation, according to the "adiabatic ionization method" ($IP_{g[X]} = \Delta H_{f[X^+]} - \Delta H_{f[X]}$). Since Koopman's theorem is based on the assumption of a "vertical" ionization and does not consider the stabilization of the system due to changes in the geometry of the cation radical, the "adiabatic" process was used for further calculations. The spin density was obtained from the difference between α- and β-electron populations. To avoid local minima pitfalls in systems with no dihedral angles, the optimization was performed at least three times using different starting structures. These were randomly generated with molecular dynamics calculations using the simulated annealing feature of HyperChem.

3. Results and discussion

3.1. Ground and excited singlet properties

The ground state molar absorption spectra of AMI-HCl and NT-HCl (Fig. 1) consist of two bands with maximum at 203 nm ($\varepsilon = 4.23 \times 10^4$ M^{-1} cm^{-1}) and 240 nm ($\varepsilon = 1.34 \times 10^4$ M^{-1} cm^{-1}), respectively. These bands show high molar absorption coefficients, because they correspond to $\pi \rightarrow \pi^*$ transitions. A lower intensity shoulder is observed in the wavelength region of 260–290 nm. The absorption spectra are similar in acetonitrile, methanol and PBS 7.4 and resemble that reported by Dall'Acqua et al. [11] and Aicart et al. [16]. These results indicate that the benzene π-system is not completely conjugated, as confirmed by the quantum chemical calculations (Fig. 2). PM3 theoretical calculations predicted several stable conformations for both AMI and NT with a maximum difference in the formation energy of 0.8 kcal mol^{-1}. For all conformations the methylene carbons at position 10 and 11 induce a torsion angle close to 63° with respect to the central ring, forcing the two benzene rings to deviate from planarity by more than 15° (see improper torsion angle in Table 1). This result is supported by the fact that the absorption spectra of AMI-HCl and NT-HCl are different to the spectra of 1,1-diphenylethylene (DPE) and 1,2-diphenylethane (1,2-DPE). The absorption spectrum of DPE extends up to 300 nm, indicating a higher resonance stabilization or a π extended conjugation of the benzene rings through the alkene double bond [17]. Even in the case of styrene, its absorption spectrum extends up to 280 nm in ethanol, due to the complete conjugation of the double bond π-electron density and the benzene ring [17]. Indeed, the spectra of AMI-HCl and NT-HCl resemble more the spectrum of DPE than that of 1,2-DPE, but this is only due to the similarity in the tri-dimensional structures of the TCAs and DPE. Nonetheless, if both model compounds are forced to have the same spatial stable conformation of AMI-HCl and NT-HCl, then the TCA spectra are similar to the spectrum of 1,2-DPE (Table 1). This suggests that the absorption properties are mainly determined by the C_{10}–C_{11}-induced conformation instead of the exocyclic double bond. To achieve similar conformations in the model molecules, the torsion angle in 1,2-DPE had to be reduced from 75 to 62° and severely restrained with a force constant of 100 kcal mol^{-1} degree^{-2}. In the case of DPE,

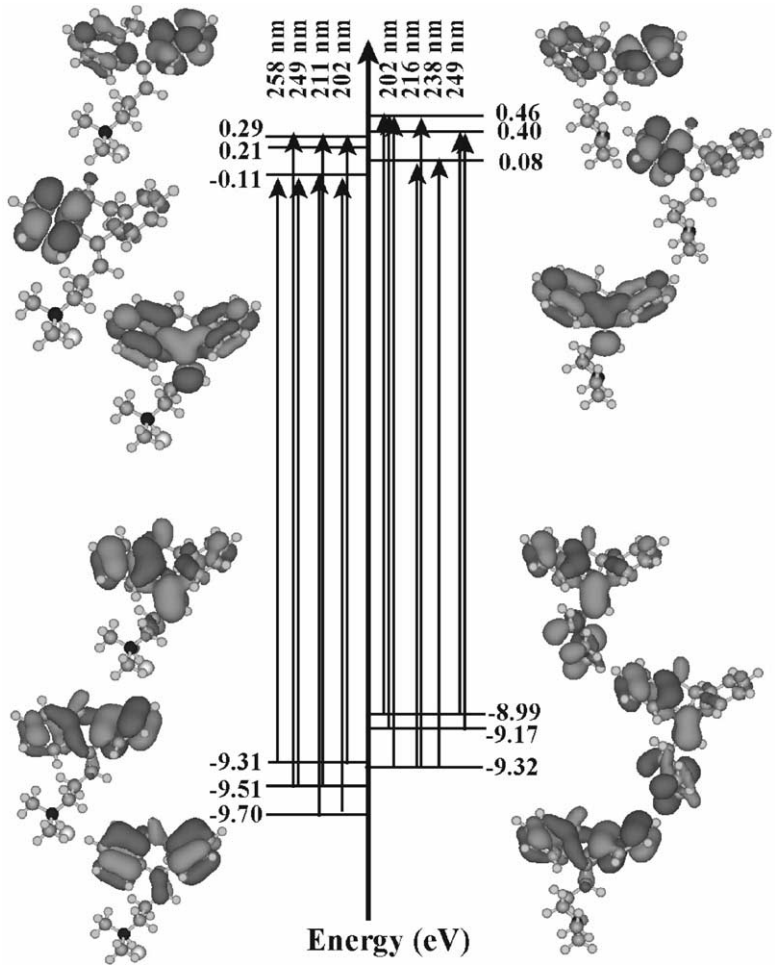

Fig. 2. Molecular orbitals involved in the UV-Vis transitions of AMI-HCl (left) and its free base (right).

Table 1
Geometrical, thermodynamical and absorption properties of the lowest energy ground and excited state conformations of AMI-HCl, NT-HCl and related compounds

Drug	Conf.	C_{10}–C_{11} torsion angle (°)	Ring improper torsion angle (°)[a]	ΔH_f (kcal mol^{-1})	μ (D)	λ_{max} [f] (nm)
AMI-HCl	S_0	62.8	164.8	20.4	4.4	202 [0.52], 211 [0.42], 249 [0.23], 258 [0.29]
	Cation	71.2	157.2	215.0	5.4	210 [0.08], 218 [0.23], 242 [0.11], 291 [0.09], 334 [0.15]
	Anion	75.1	158.9	6.1	5.9	211 [0.13], 217 [0.25], 258 [0.08], 291 [0.28], 322 [0.06]
	Product[b]	75.3	162.5	55.7	1.2	226 [0.78], 232 [0.43], 245 [0.12]
NT-HCl	S_0	62.8	164.9	22.9	4.5	202 [0.54], 211 [0.43], 248 [0.22], 258 [0.28]
	Cation	71.2	156.5	218.0	5.1	211 [0.08], 218 [0.23], 242 [0.11], 256 [0.09], 291 [0.09], 335 [0.15]
	Anion	75.3	158.9	8.1	4.6	211 [0.13], 217 [0.25], 258 [0.08], 291 [0.28], 322 [0.06]
DPE	S_0	–	99.6	65.3	0.05	204 [0.19], 255 [0.36], 261 [0.42]
	S_0[c]	–	177.0	65.1	0.02	242 [0.42], 258 [0.39]
1,2-DPE	S_0	75.1	107.9	37.7	0.2	247 [0.79]
	S_0[d]	62.3	140.4	38.0	0.2	192 [0.41], 217 [0.03], 234 [0.34], 261 [0.23]

[a] Angle between the planes containing each benzene.
[b] Stable product in Scheme 1, previously identified by Epling et al. [12].
[c] The torsion angle of the C_8 containing ring and the double bond was restrained to 58° to resemble the conformation of AMI and NT.
[d] The C_{10}–C_{11} torsion angle was restrained to 62° to resemble the conformation of AMI and NT.

the improper torsion angle had to be increased from 99 to 165° and restrained with the same force constant. The hyperconjugation in the first case reproduced the AMI-HCl and NT-HCl spectra better than the π-conjugation in DPE. Thus, it can be concluded that AMI-HCl and NT-HCl present ground state absorption properties similar to those of a normal non-conjugated benzene system separated by sp^3 carbons with an improper torsion angle of 140°.

Deprotonation of the amino group does not change the TCA absorption properties very much. The only remarkable feature of the AMI and NT electronic transitions is that the corresponding orbitals have some contributions from the NH_2-atomic orbitals (Fig. 2). According to the PM3 results, the 254 nm transition has charge transfer character because the electron density at the terminal amino group decreases on excitation. This decrease of electron density should eventually favor the demethylation process as will be discussed later.

The emission spectra of AMI-HCl and NT-HCl in PBS 7.4 consisted of a low intensity broad band with maximum at 360 nm. A 17 nm blue shift in the emission maximum was observed in methanol and acetonitrile (Fig. 1). The emission spectrum was determined using 280 nm excitation wavelength, which corresponds to the red side region of the absorption band. To obtain an absorbance of 0.10 units at 280 nm, a concentration of 129 μM was required. This concentration was well below the critical aggregation concentration of 43.7 mM at pH of 7.4, as determined from conductance measurements [16]. The fluorescence quantum yield is very low ($\phi_f \approx 0.002$–0.004) as expected for polyenes or alkenes in the solvents tested. For comparison purposes, a 0.003 fluorescence quantum yield has been reported for DPE in cyclohexane [18]. Moreover, for *cis*-stilbene the fluorescence quantum yield is close to zero, while for *trans*-stilbene is 0.05 [19]. Therefore, AMI-HCl and NT-HCl resemble more the *cis*-stilbene fluorescence properties. This is supported by the observation that the orbital responsible for the fluorescence (optimized S_1 state) is completely conjugated with the atomic orbitals of the stilbenyl moiety (data not shown). The calculated S_1 conformation presents a longer double bond (>1.45 Å) than the S_1-Franck–Condon state (<1.40 Å). The low fluorescence yield of *cis*-stilbene has been interpreted in terms of the steric interactions between the phenyl groups that induce a twist around the central carbon double bond. This twist results in an enhanced internal conversion rate constant [19]. It can be expected that a similar argument applies to AMI-HCl or NT-HCl because the *N*-methyl aminopropyl side chain substitution can also induce steric interactions with the phenyl groups resulting in a twist around the dibenzocycloheptene exocyclic bond. This can explain the observed low fluorescence yield for AMI or NT derivatives.

Attempts were made to determine the fluorescence lifetime of AMI-HCl by measuring its frequency response, but the measured value had a large uncertainty. This was due to the low emission yield and the low intensity of the excitation lamp at 280 nm (see Section 2). However, radiative rate constants (k^0) can be approximated by the Strickler–Berg relationship (Eq. (1)) [19],

$$k^0 = 3 \times 10^{-9} \tilde{\nu}_0^2 \int \varepsilon(\tilde{\nu})\, \mathrm{d}\tilde{\nu} \quad (1)$$

where $\tilde{\nu}_0$ is the energy (cm^{-1}) corresponding to the maximum wavelength of absorption and the integral is the area under the curve of the molecular absorption coefficient versus the wavenumber. The calculated inherent radiative rate constant (k^0) for AMI-HCl was $3.07 \times 10^8\ s^{-1}$. The theoretical oscillator strength of 0.25 calculated from the experimental absorption spectrum by using the relation $4.3 \times 10^{-9} \int \varepsilon\, \mathrm{d}\tilde{\nu}$ [19] is in excellent agreement with the f of 0.23 determined by quantum chemical calculations for the 249 nm transition reported in Table 1. Fluorescence lifetimes for phenylethylenes of less than 1 ns in fluid solutions have been reported. For example, for *trans*-stilbene the τ_f is 75 ps [20]. Therefore, we expected that the AMI-HCl fluorescence lifetime should be of the order of fractions of nanoseconds. Furthermore, the k^0 ($4.29 \times 10^6\ s^{-1}$) calculated from the fluorescence quantum yields of AMI-HCl and the measured lifetime of 0.7 ns is much smaller than the k^0 determined from Eq. (1). This suggests that although the absorption corresponds to an allowed Franck–Condon transition, the emission is forbidden and originates from a non-Franck–Condon state. This emission probably originates from a perpendicular conformation of the exocyclic double bond, similar to that proposed for other alkylethylenes molecules [19].

3.2. Transient absorption spectroscopy

3.2.1. Excitation at 266 nm

The 266 nm nanosecond transient absorption spectra of a nitrogen-saturated AMI-HCl solution (0.5 mM PBS 7.4) is shown in Fig. 3. Similar spectra were observed for NT-HCl. The spectra consisted of two bands, one extending from 400 to 750 nm and peaking at 720 nm; and another in the UV region with maximum at 330 nm. The UV band showed an increase in absorbance during the first 0.6 μs and then decayed with a lifetime of 25 μs. The short-lived species absorbing in the visible region was quenched by O_2 and N_2O. Both additives are efficient electron scavengers and react with rate constants of 1.9×10^{10} and $9.1 \times 10^9\ M^{-1}\ s^{-1}$, respectively [21]. Thus, this transient absorption was assigned to the solvated electron. The solvated electron decay lifetime decreased linearly with the ground state concentration of AMI-HCl or NT-HCl, indicating the formation of the corresponding anion radical according to Eq. (2).

$$\mathrm{TCA} + \mathrm{e_{ac}}^- \rightarrow \mathrm{TCA}^{\bullet -} \quad (2)$$

From a plot of the pseudo-first-order rate constant of the electron decay versus the ground state concentration, bimolecular rate constants of 6.5×10^9 and $5.5 \times 10^9\ M^{-1}\ s^{-1}$ were calculated for the electron addition of AMI-HCl and NT-HCl, respectively. This similarity reflects once more

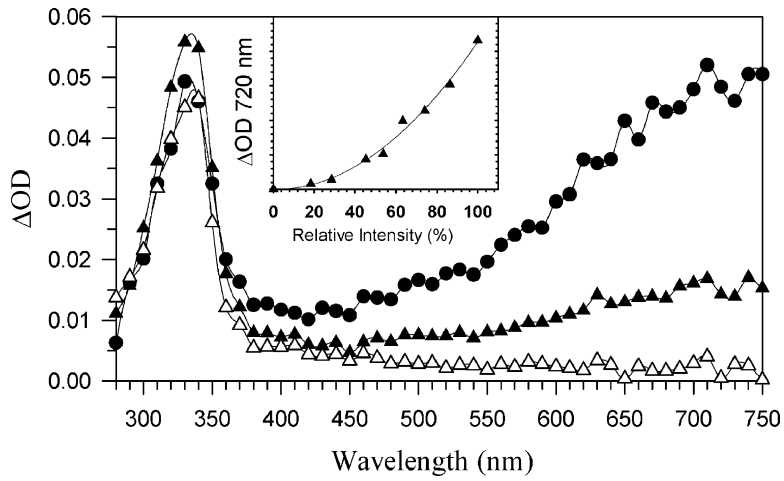

Fig. 3. Transient absorption spectra of AMI (0.50 mM) in nitrogen-saturated 10 mM PBS 7.4 solution measured at 97 ns (●), 486 ns (▲) and 3.9 μs (△) after the 266 nm laser pulse excitation. Inset: Laser power curves for yields of solvated electrons (transient absorption signal measured at 720 nm immediately after the laser pulse).

their structural and reactivity similarities. From the absorbance of the solvated electron at 720 nm (measured 97 ns after the laser pulse), the electron molar absorption coefficient at this wavelength and the TCA analytical concentrations (0.50 mM), similar photoionization yields of 0.5 and 0.4% were calculated for AMI-HCl and NT-HCl, respectively (Eq. (3)).

$$\%\mathrm{PI} = \frac{100\,\Delta\mathrm{OD}_{720}}{\varepsilon_{720}[\mathrm{drug}]_0} \tag{3}$$

The effect of the laser intensity on the solvated electron yield was further examined. A plot of the signal intensity at 720 nm at the end of the laser pulse against the laser energy shows an upward curvature at high laser doses (Fig. 3). This non-linear power dependence is a clear indication of a multiphoton processes with the yield of the solvated electron being proportional to the square of the laser fluence. A value of 2.01 was estimated from the power curve. The ionization potentials of these molecules in aqueous solution ($IP_{solution}$) were calculated using Eq. (4) [22] and the results are included in Table 2.

$$\mathrm{IP}_{solution} = \mathrm{IP}_g + P_+ + V_0 \tag{4}$$

In this equation, IP_g is the ionization potential in the gas phase, P_+ is the adiabatic electronic polarization energy of the medium by the positive ion and V_0 is the ground state energy of the "quasi-free" electron in the liquid relative to the electron in vacuum. The IP_g values were determined from the difference in formation enthalpies, as described in Section 2. The value of P_+ was obtained using Born's equation: $P_+ = -e'(\varepsilon - 1)/2r^+\varepsilon$, where $e' = e^2/4\pi\varepsilon_0$ and ε, is the solvent optical dielectric constant and r^+ is the radius of the radical cation (calculated from the molecular volume, which was obtained using the grid method implemented in HyperChem). The following values for V_0 were used: −1.5 for acetonitrile [23,24], −1.3 eV for water [25] and −1.0 for methanol [25]. The gas phase ionization potential calculated values (Table 2) are in an excellent agreement with the

Table 2
Ionization and oxidation potentials of AMI-HCl, NT-HCl and related compounds in water ($\varepsilon = 78.5D$), methanol ($\varepsilon = 32.6D$) and acetonitrile ($\varepsilon = 37.5D$)

Molecule	Volume (Å^3)	IP_{gas} (eV)		P_+ (eV)			$IP_{solution}$ (eV)[a]			E_{ox} (V)	
		A[b]	B[c]	H_2O	CH_3OH	CH_3CN	H_2O	CH_3OH	CH_3CN	CH_3OH	CH_3CN
AMI-HCl	969.2	9.3	8.4[d]	1.16	1.14	1.14	5.94	6.26	5.76	1.72	1.90
NT-HCl	926.2	9.3	8.4[e]	1.18	1.15	1.16	5.92	6.25	5.74	1.72	1.90
AMI	901.5	9.1	7.9	1.19	1.16	1.17	5.41	5.74	5.23	1.83	1.93
NT	857.6	9.2	8.3	1.21	1.18	1.19	5.79	6.12	5.61	1.76	1.93
DPE	626.5	9.1	8.6	1.34	1.31	1.32	5.96	6.29	5.78	–	–
1,2-DPE	642.2	9.4	9.0	1.33	1.30	1.31	6.37	6.70	6.19	–	–

[a] Calculated with the "adiabatic" gas ionization potential.
[b] Obtained from Koopman's theorem.
[c] Calculated with the formation enthalpy of the molecule and the corresponding cation.
[d] Experimental value 8.32 ± 0.07 [26,27].
[e] Experimental value 8.39 ± 0.11 [26].

experimental values obtained from charge transfer spectra for AMI [26,27] and NT [26]. All other calculated values are summarized in Table 2, including Koopman's ionization potentials. As mentioned before, the relative high values of this quantity can be attributed to the non-stabilization of the cation radical. Values of $IP_{solution}$ greater than 5.2 eV were estimated for all molecules in all solvents. Since this $IP_{solution}$ is larger than the 266 nm laser photon energy (4.7 eV), the molecule must absorb two photons in order to produce states with energies exceeding 5.2 eV. The nature of the intermediate state from which the photoionization occurs cannot be established because upon direct 266 nm laser excitation of the TCA solutions, a band that could be assigned to a triplet–triplet absorption was not observed. Furthermore, the relaxed singlet state presented a short lifetime. Because the radicals produced under direct excitation could obscure transient with lifetimes smaller than 200 ns, photosensitization studies were performed to obtain a better time and spectral resolution.

Cyclic voltammograms of AMI-HCl and NT-HCl and their free bases show two oxidation peaks (Fig. 4). The oxidation peak at a lower positive potential (1.05 and 1.42 V for the free base and for NT-HCl/AMI-HCl in acetonitrile, respectively) is associated to the amino group by comparison with *N*-methylaminopropyl as standard and also with PTL-HCl and its free base [28]. Both NT and AMI have identical oxidation potentials in methanol (1.72 V) and acetonitrile (1.90 V) corresponding to the dibenzocycloheptene moiety. Because the potentials measure the ease of oxidation, the oxidation ability in methanol is higher than in acetonitrile. However, the magnitude of the oxidation potentials in methanol and acetonitrile does not follow the trend of the quantum theoretical calculated ionization potentials. Nevertheless, this difference is within the error of the theoretical ionization potential (±0.5 eV). Also, this difference can be explained in terms of specific solvent solute interactions not taken into consideration by the Born's equation. This equation is based on the simple model of a spherical ion with a single point charge at its center and only takes into consideration the solvent polarity function.

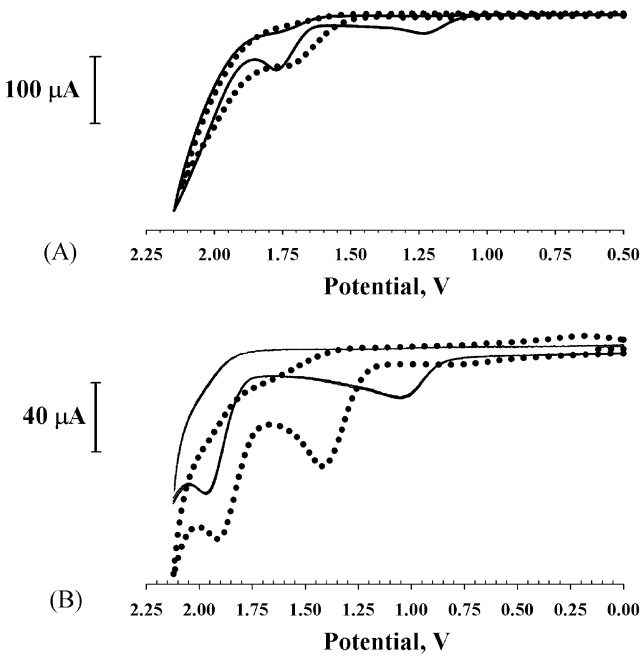

Fig. 4. Cyclic voltammograms of nortriptyline (3.0 mM) and 0.1 M TBAP at scan rate of 100 mV s^{-1} in (A) methanol and (B) acetonitrile. NT-free base (solid line) and NT-HCl (dotted line).

The observation of a hydrated electron band in the laser flash photolysis implies the formation of a geminate radical cation. The UV band with maximum at 330 nm was observed in nitrogen, air and N_2O-saturated solutions. The only observable difference under those conditions was that in the presence of air and N_2O there was no increase in the absorbance at short times. Moreover, a decrease in the absorbance intensity at 330 nm of 18 and 56% was observed under an air atmosphere and in N_2O-saturated PBS 7.4 solutions containing 0.1 M *t*-butanol, respectively, compared to nitrogen-saturated solutions under similar laser intensity and ground state concentrations. This suggests that at these wavelengths this absorption band has contributions from species for which the solvated electron is a precursor. Such species could be an AMI or NT electron adduct formed through the reaction of a ground state molecule with the hydrated electron with nearly diffusion controlled rate constant (Eq. (2)). Since oxygen and N_2O are efficient electron scavengers, the formation of the radical anion can be disregarded under those conditions. Therefore, the band at 330 nm must also have contributions from the cation radical. To corroborate this statement, the transient intermediates were further studied under oxidative and reductive conditions as will be discussed later in Sections 3.2.3 and 3.2.4.

3.2.2. Photosensitization studies

As discussed above, the amitriptyline chromophore presents similar photophysical properties and electronic configuration to those of DPE or 1,2-DPE. Thus, similar excited state properties are expected for AMI derivatives. The quantum yields of intersystem crossing for phenylethylenes are in general low and the lifetimes of arylethylenes triplets at room temperature are in the nanosecond rather than in the microsecond range [18]. For example, triplet lifetimes in the 100 ns range have been reported for styrenes, stilbene, 1,1-diphenyl-2-methylpropene and other derivatives using photosensitization by transient absorption and photoaccoustic calorimetry [18,29]. High energy triplet donors such as benzophenone, thioxanthone and xanthone were used to sensitize the triplet state of 1-1-diphenylethylene, triphenylethylene and tetraphenylethylene [18]. The latter transient species absorb in the wavelength region of 360–400 nm region with lifetimes in the 30–200 ns range, where the longer lifetimes correspond to the more substituted ethylenes. The deactivation of the phenylethylenes triplet has been proposed to occur through the internal conversion of the perpendicular triplet to the ground state via

a twisting of the central double bond [18,29]. Photosensitization studies of AMI and NT were performed using thioxanthone. The ^{3}TX* triplet excited state absorption measured at 630 nm was quenched by AMI-HCl, NT-HCl and AMI with rate constants of 1.47, 2.55 and $4.1 \times 10^9\ M^{-1}\ s^{-1}$, respectively, as determined by Stern–Volmer plot. These rate constants show that the TCA-free base is more reactive than the protonated form. For comparison purposes, the reported quenching rate constant for the reaction of ^{3}TX* with DPE, triphenylethylene and tetraphenylethylene in benzene are 5.5, 7, and $5 \times 10^9\ M^{-1}\ s^{-1}$, respectively [18].

The transient absorption spectra observed after the 355 nm laser excitation of TX (0.05 mM) in a solution containing AMI-HCl (10.0 mM) are shown in Fig. 5A. The spectrum recorded 28 ns after the laser pulse presents transient absorption bands with maxima at 320 and 625 nm and a depletion region due to the TX ground state absorption in the 370–400 nm range. The 320 and 625 nm bands disappeared in less than 1 μs and the 320 nm band maximum shifted to 330 nm with time. The transient absorption spectrum measured at 4000 ns for the TX triplet quenching by AMI-free base is shown in Fig. 5B. This spectrum shows the presence of the thioxanthyl ketyl radical band in the 400–500 nm region in addition to the AMI$^{\bullet+}$ in the 330 nm region. Furthermore, the kinetic trace at 420 nm shows an increase in absorbance with a lifetime of 0.6 μs which then decays with a lifetime of 10.6 μs.

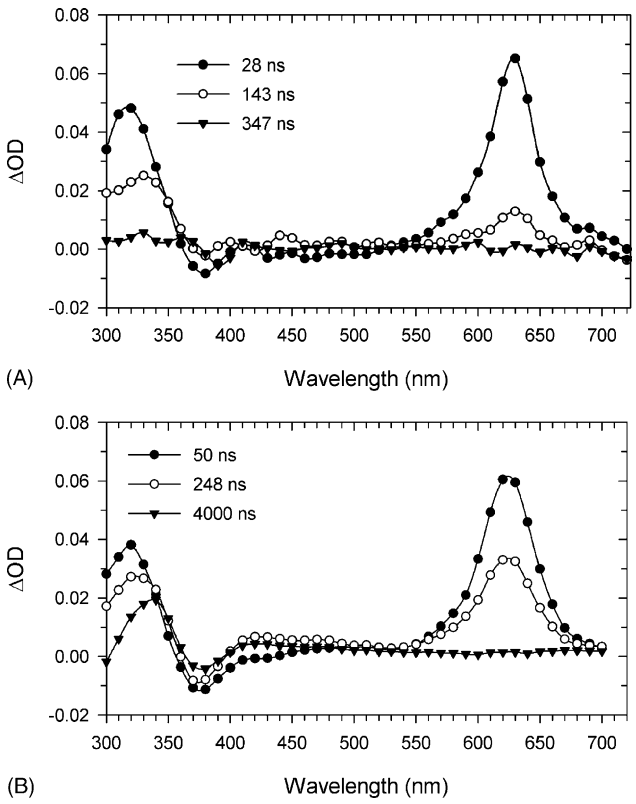

Fig. 5. Transient absorption spectra with 355 nm laser excitation of TX (0.05 mM) in nitrogen-saturated acetonitrile solutions in the presence of (A) AMI-HCl, 10.0 mM and (B) AMI-free base, 0.75 mM.

The kinetic traces observed at 330 nm under different experimental conditions are shown in Fig. 6. The thioxanthone triplet state is produced within the laser pulse and absorbs at 330 nm (Fig. 6A). In the absence of a quencher, the transient absorption due to the decay of ^{3}TX* remains constant during the experimental timescale. On the other hand, when the AMI-free base was added, a rapid decay of ^{3}TX* with lifetime of 270 ns and a long-lived residual absorption ($\tau > 5.0$ μs) were observed (Fig. 6B). The difference in absorbance between the residual absorption and the pre-laser baseline at 330 nm under those conditions increased proportionally with AMI-free base concentration (data not shown). In the presence of AMI-HCl (10.0 mM) an increase in absorbance with $\tau = 25$ ns followed by a decay with $\tau = 171$ ns at 330 nm were observed (Fig. 6C), while at 630 nm, the ^{3}TX* decayed with lifetime of 65 ns. Similar results were observed for NT-HCl. These kinetics results indicate that the quenching of the ^{3}TX* depends on the protonation state of the TCA amino group. The ^{3}TX* state is known to be photoreduced by amines via a charge transfer or exciplex intermediate to thioxanthyl ketyl radical [30,31]. The thioxanthyl ketyl radical absorbs in the 400–500 nm with maxima at 425 nm. Therefore, the transient absorption spectrum resulting from the photoexcitation of TX in the presence of the TCA-free base can be explained in terms of an electron transfer mechanism producing radical species (Fig. 5B). These results are in accordance with the observed oxidation ability of protonated AMI or NT and their corresponding free base. The probability of an electron transfer process was estimated by the Rehm–Weller equation (Eq. (5)) [32],

$$\Delta G = E\frac{D}{D^{\bullet+}} - E\frac{A}{A^{\bullet-}} - \frac{e^2}{\varepsilon a} - E_{00} \qquad (5)$$

where ΔG is the free energy for the electron transfer, $E(D/D^{\bullet+})$ is the oxidation potential of the donor, $E(A/A^{\bullet-})$ is the reduction potential of the acceptor, E_{00} is the energy of the excited state and $e^2/\varepsilon a$ is the Coulombic term, which is small for acetonitrile (0.5 eV) and can be disregarded. For TX in acetonitrile solution ($(E(A/A^{\bullet-}) = -1.66$ V versus SCE and $E_{00} = 274.4\ kJ\ mol^{-1}$) it was concluded that electron transfer can be exergonic for any donor with $E(D/D^{\bullet+}) < 1.18$ V [30]. The amino group oxidation potential of the TCA deprotonated and protonated forms in acetonitrile were determined to be 1.05 and 1.42 V, respectively (Fig. 4B). From these values it can be concluded that electron transfer between ^{3}TX* and the TCA-free bases is exergonic ($\Delta G = -13.5\ kJ\ mol^{-1}$). On the other hand, for the TCA-HCl the electron transfer process is endergonic ($\Delta G = 22.2\ kJ\ mol^{-1}$). These results clearly support the electron transfer mechanism proposed for the reaction of the ^{3}TX* and the TCA-free base. However, the kinetic behavior observed for the ^{3}TX* and TCA-HCl system is more complex. The absorbance increase at short times after the pulse can be assigned to an energy transfer process because no radical ions were observed. If the radical ions of the TCA were formed, their absorption should have persisted

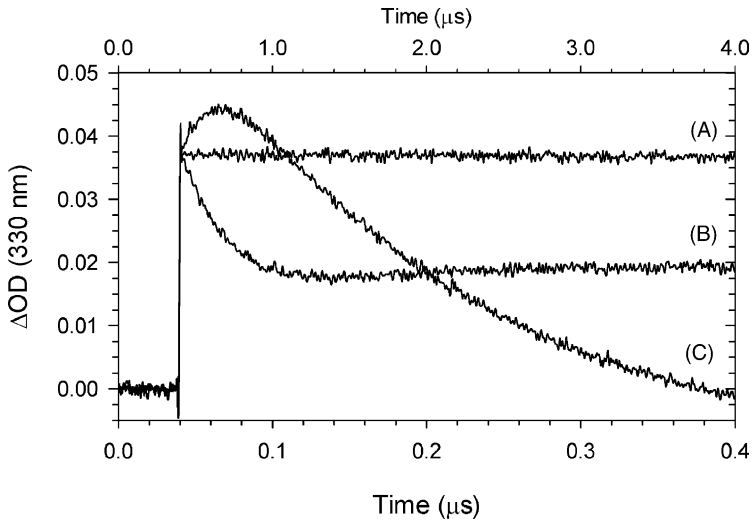

Fig. 6. Transient kinetic traces measured at 330 nm with 355 nm laser excitation of TX (0.05 mM) in nitrogen-saturated acetonitrile; (A) TX alone, (B) plus AMI, 1.0 mM and (C) AMI-HCl, 10.0 mM. Note that the top scale corresponds to curve B.

for longer than 5 μs (see below). This assignment can also be justified based on the previously reported photosensitization studies of phenylethylenes derivatives [18,29]. The triplet lifetime for AMI-HCl or NT-HCl were difficult to determine because ^{3}TX* also absorbs at 330 nm.

Nonetheless, triplet lifetimes in the 25–130 ns range can be extrapolated for these TCA. This short lifetime is attributed to the twisting conformation of the exocyclic double bond as previously proposed for the phenylethylenes and other olefins [18,29]. This state can be a possible precursor for the absorption of a second photon to produce the radical cation. Two observations sustain this hypothesis; (a) the lifetime is long enough to allow for the absorption of a nanosecond laser pulse and (b) the intersystem crossing of AMI and NT are small under direct excitation, thus resulting in low photoionization yields. To corroborate that TX can photosensitize the TCA, experiments were performed using protriptyline hydrochloride. The protriptyline (PTL-HCl) triplet excited state had been characterized recently by our group [28]. The protriptyline triplet state absorbs at 420 nm ($\epsilon_T = 16{,}000\ M^{-1}\ cm^{-1}$) and has a triplet energy close to 53 kcal mol^{-1}. In addition, it has the same *N*-methylamino propyl side chain. It was observed that the ^{3}TX* photosensitizes the PTL-HCl or its free base triplet state (data not shown). The reported oxidation potential for the amino side chain of PTL-HCl and its free base is higher than 1.20 V [28]. Therefore, an endergonic electron transfer processes is expected for the ^{3}TX* quenching of PTL. Thus, it can be established that the ^{3}TX* quenching mechanism by TCA depends on the amino side group oxidation potential.

3.2.3. Generation of AMI and NT radical cation via reduction of $SO_4^{\bullet-}$ radical

To verify the presence of the oxidized radical at 330 nm, the laser photolysis of an N_2-saturated aqueous solution containing 5.0 mM potassium peroxydisulfate and 0.20 mM AMI-HCl at pH 7.4 was performed [33]. Under these conditions, most of the light is absorbed by the $S_2O_8^{2-}$ ions to generate the one-electron oxidant sulfate radical anion, which rapidly reacts with the TCAs to produce their corresponding radical cations according to the following mechanism:

$$S_2O_8^{2-} \xrightarrow{h\nu} SO_4^{\bullet-} + SO_4^{2-} \quad (6)$$

$$TCA + SO_4^{\bullet-} \rightarrow TCA^{\bullet+} + SO_4^{2-} \quad (7)$$

The transient absorption spectrum obtained under those conditions is depicted in Fig. 7A. Immediately after the laser

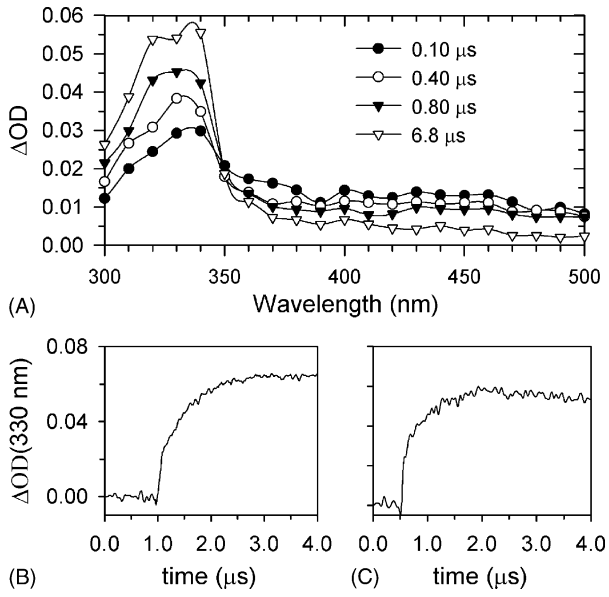

Fig. 7. (A) Transient absorption spectra of AMI (0.20 mM) and $K_2S_2O_8$ (5.0 mM) in nitrogen-saturated PBS 7.4 solution with different delay times after the 266 nm laser pulse excitation. Inset: Kinetic traces measured at 330 nm in the presence of (B) $K_2S_2O_8$ (5.0 mM) and (C) $K_4Fe(CN)_6$ (0.25 mM).

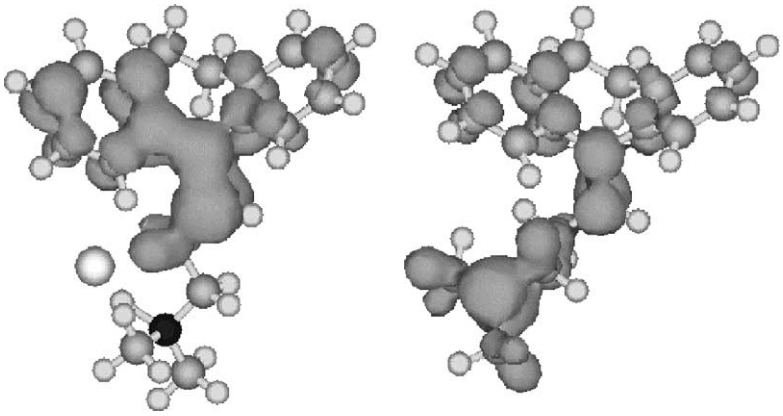

Fig. 8. PM3 Spin density of $AMI^{\bullet+}$ protonated (left) and unprotonated (right).

pulse, an increase in absorbance with risetime of 0.45 μs at 330 nm was observed and was assigned to the AMI-HCl radical cation (Fig. 7B). This radical cation decayed through a first-order kinetics with $\tau = 20$ μs, similar to the lifetime obtained under direct excitation of an N_2O-saturated aqueous AMI-HCl solution. The corresponding $SO_4^{\bullet-}$ transient absorption was observed at 450 nm. The bimolecular rate constant for the reaction between AMI-HCl and $S_2O_8^{2-}$ was calculated to be $4.4 \times 10^8\ M^{-1}\ s^{-1}$.

Theoretical PM3 quantum chemical calculations indicate that the unpaired spin density in the radical cation is distributed between the double bond and the ring with the smallest torsion angle, i.e. the electron is practically withdrawn from the exocyclic carbon double bond (Fig. 8). If the TCA is not protonated, on the other hand, the electron can be withdrawn from the amino group. In this case, the radical cation spin density is distributed between this group and the exocyclic double bond. This explains the difference found by Epling et al. [12] regarding the higher reactivity of unprotonated versus protonated AMI.

Based on these findings, the mechanisms presented in Schemes 1 and 2 are proposed for the formation of the main stable photoproducts identified by these authors [12]. In Scheme 1, the radical cation is the primary radical intermediate. The radical cation can undergo the proposed 1,3-sigmatropic rearrangement. The 1,3-hydrogen shift must occur within picoseconds and the participating electron can be either the solvated electron or an intra or intermolecular charge transfer interaction with the terminal amino group. In both cases, these processes could occur within the lifetime of the $TCA^{\bullet+}$ (≈20 μs).

In Scheme 2, the radical cation charge is located on the amino group of the unprotonated form of TCA. The formation of nortriptyline by demethylation from the unprotonated species can be predicted by PM3 theoretical results (Fig. 8). It also explains the formation of the aldehyde by the hydrolysis of the terminal amino group.

3.2.4. Generation of AMI and NT radical anions

To verify if the radical anion also absorbs in the 330 nm wavelength region, the photolysis of a nitrogen-saturated aqueous solution containing 0.25 mM $K_4Fe(CN)_6$ and 0.20 mM AMI at pH 7.4 was performed [34]. This experimental approach can be justified based on (a) the higher absorbance of $Fe(CN)_6^{4-}$ at 266 nm than AMI-HCl under the experimental conditions, (b) the very small photoionization yield of AMI-HCl and NT-HCl under direct excitation and (c) the close to ten fold ratio of the reaction rates of electron scavenging by AMI-HCl to the electron–electron reaction rate. Under these conditions, the $Fe(CN)_6^{4-}$ was photoionized with 266 nm laser light producing a high concentration of solvated electron ($\phi_{e^-} = 0.50$), which then reacts with ground state AMI-HCl yielding the corresponding radical anion ($AMI^{\bullet-}$). The results showed an increase

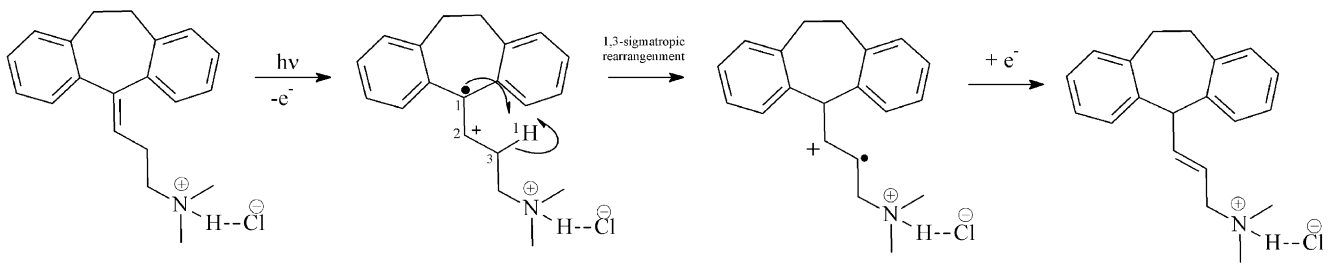

Scheme 1.

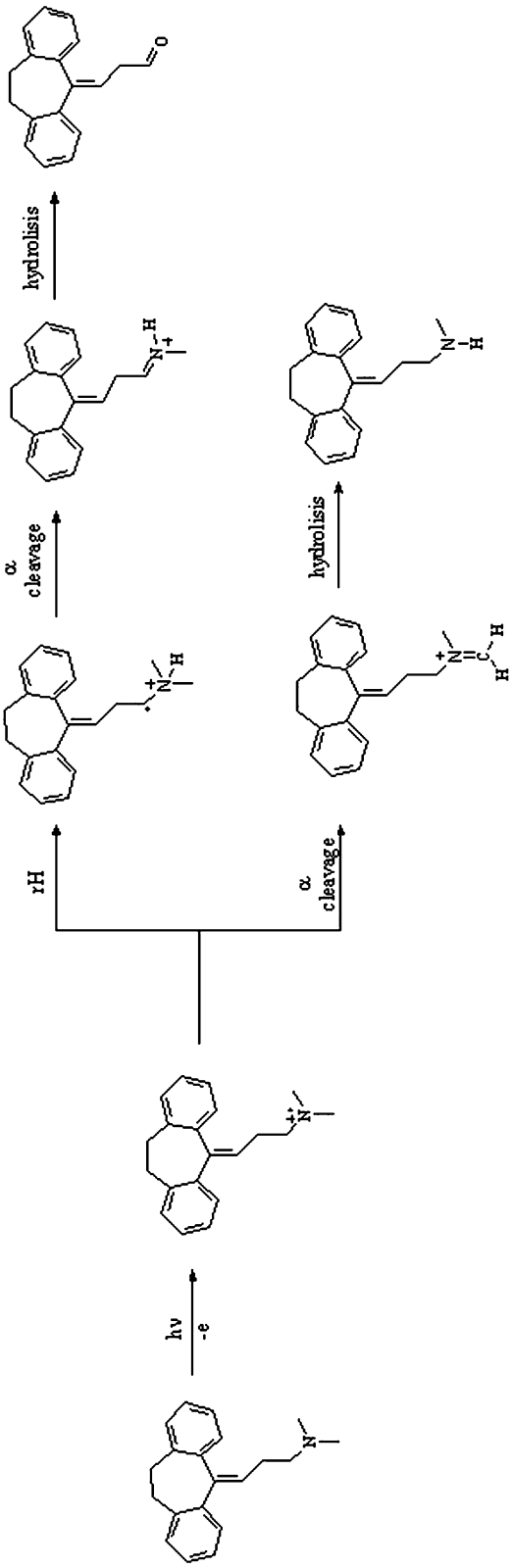

Scheme 2.

in absorbance at 330 nm after the laser pulse with risetime of 0.43 μs (Fig. 7C). Once formed, the radical anion decays with a lifetime of 12 μs, which is shorter than that observed for the radical cation. Also, the solvated electron lifetime measured at 720 nm in the presence of AMI-HCl was reduced by a factor of 2. From the initial solvated electron absorbance at 720 nm and its molar absorption coefficient (18,500 M^{-1} cm^{-1}) [35], an electron concentration of 15 μM was calculated. Assuming that all the solvated electrons react with AMI-HCl, an equal concentration of radical anions is produced. Therefore, using the measured maximum transient absorbance at 330 nm and the radical anion concentration, a molar absorption coefficient of 5.3×10^3 M^{-1} cm^{-1} at 330 nm was calculated for $AMI^{\bullet -}$. Theoretical calculations predict a blue shift of 8 nm for both anion radicals, relative to the 330 nm band of the corresponding radical cation. Nonetheless, these calculations are not very reliable, because they had almost 25% of spin contamination for species with multiplicity of 2.

4. Conclusions

In this report, we show that the primary species produced by the 266 nm laser flash photolysis of AMI-HCl and NT-HCl solutions are the solvated electron, formed through a biphotonic photoionization process, and the corresponding radical cation. The results of the steady-state photolysis of the free base of AMI and NT reported by Epling et al. [12] provided evidence for the photofragmentation of these molecules and for the formation of several photoproducts. The mechanism proposed by these authors involved the formation of a radical cation and an anion of the drugs through an intermolecular exciplex or intramolecular step. Our results do not provide direct evidence of an exciplex formation. However, we could not discard the possibility that the primary radicals produced upon direct laser photolysis further react with ground state molecules and produce secondary species, and eventually, the previously observed photoproducts. In addition, radical rearrangements of the primary radical ions, as proposed in Schemes 1 and 2, could lead to the final photoproducts. The identification of the AMI and NT primary radicals confirms the postulated Type I photosensitizing properties of AMI reported by Dall'Acqua et al. [11]. These authors also stated that although this drug induces photosensitizing reactions in humans, this adverse effect is far less common than those observed for other class of compounds such as the phenothiazines derivatives. Our results totally agree with that observation. Moreover, they also confirm that the molecular structure of the different antidepressive drugs governs their photophysical properties, and thus, their phototoxic damaging effects. This is clearly illustrated by comparing AMI, NT, and protriptyline. The difference between both molecules is the position of the alkene bond in the dibenzocycloheptene moiety. In protriptyline, the double bond is endo at the C_{10} and C_{11} carbons of the AMI or NT dibenzocycloheptene moiety. This alkene substitution drastically changes the corresponding photophysical properties. Recent reports from our laboratory demonstrated that protriptyline shows a high fluorescence quantum yield and the presence of a triplet state [28]. In addition, the protriptyline triplet state was shown to produce singlet oxygen through energy transfer. Also, a two photon photoionization process was found for protriptyline. However, AMI showed no singlet oxygen production, implying the absence of the participation of triplet state in its phototoxicity. On the other hand, the oxidation and theoretical ionization potentials for AMI-HCl, NT-HCl and protriptyline hydrochloride are similar. Thus, the alkene position is definitely the factor that drastically changes the photochemical and photophysical properties of these derivatives. Finally, several reports have proposed a possible interaction between AMI and the CYP450 enzyme [6,7]. This enzyme participates in an electron transfer process in which one of the observed radical intermediates in this study could participate in promoting cellular damaging effects.

Acknowledgements

This work has been supported in part by NIH-MBRS Grant S06GM08216 to UPR-Humacao. R. Oyola also appreciate the financial support from GAAN fellowship program from the Dept. of Education, USA and the Puerto Rico Industrial Development Company.

References

[1] G.M. Bump, B.H. Mulsant, B.G. Pollock, S. Mazumdar, A.E. Begley, M.A. Dew, C.F. Reynolds, Depress. Anxiety 13 (2001) 38.
[2] B.H. Mulsant, R.A. Sweet, J. Rosen, B.G. Pollock, G.S. Zubenko, T. Flynn, A.E. Begley, S. Mazumdar, C.F. Reynolds, J. Clin. Psychiatry 62 (2001) 597.
[3] K. Venkatarishnan, J. Schmider, J.S. Harmatz, B.L. Ehrenberg, M.L. Von, J.A. Graf, P. Mertzanis, K.E. Corbett, M.C. Rodríguez, R.I. Shader, D.J. Greenblatt, J. Clin. Pharmacol. 41 (2001) 1043.
[4] M.G. Casarotto, D.J. Craik, J. Phys. Chem. 96 (1992) 3146.
[5] D.J. Craik, M.G. Casarotto, J. Phys. Chem. 95 (1991) 7093.
[6] P. Ghahramani, S. Ellis, M. Lennard, L. Ramsay, G. Tucker, Br. J. Clin. Pharmacol. 43 (1997) 137.
[7] O. Olesen, K. Linnet, Pharmacology 55 (1997) 235.
[8] V. Narurkar, B. Smoller, C. Hu, E. Bauer, Arch. Dermatol. 129 (1993) 474.
[9] S. Taniguchi, T. Hamada, Am. J. Hematol. 53 (1996) 49.
[10] H.J. Milionis, A. Skopelitou, M.S. Elisaf, Postgrad. Med. J. 76 (2000) 361.
[11] F. Dall'Acqua, V. Miolo, D. Vedaldi, Farmaco 55 (2000) 211.
[12] G.A. Epling, M.T. Sibley, T.T. Chou, A. Kumar, Photochem. Photobiol. 47 (1988) 491.
[13] N.J. Turro, G.J. Kavarnos, Chem. Rev. 86 (1986) 401–449.
[14] J.R. Lakowicz, Principles of Fluorescence Spectroscopy, Plenum Press, New York, NY, 1983.
[15] J. Demas, G. Crosby, J. Phys. Chem. 75 (1971) 991.
[16] E. Aicart, E. Junquera, J.C. Romero, Langmuir 17 (2001) 1826.

[17] J.B. Lambert, H.F. Shurvell, D.A. Lightner, R.G. Cooks, Organic Structural Spectroscopy, Prentice-Hall, Englewood Cliffs, NJ, USA, 1998.
[18] H. Gorner, J. Phys. Chem. 86 (1982) 2028.
[19] N.J. Turro, Modern Molecular Photochemistry, University Science Book, California, 1991.
[20] R. Dabestani, I.N. Ivanov, Photochem. Photobiol. 70 (1999) 10.
[21] M. Anbar, P. Neta, Int. J. Appl. Radiat. Isot. 18 (1967) 493.
[22] T. Ogawa, T. Ogawa, K. Nakashima, J. Phys. Chem. 102 (1998) 10608.
[23] J.L. Faria, S. Steenken, J. Phys. Chem. 97 (1993) 1924.
[24] H.M. Murgida, G.M. Bilmes, R. Era-Belsells, Photochem. Photobiol. 64 (5) (1996) 777.
[25] E. Amouyal, S. Bernas, D. Grand, Faraday Discuss. Chem. Soc. 74 (1982) 147.
[26] A. Fulton, L.E. Lyons, Aust. J. Chem. 21 (1968) 873.
[27] A.P. Poltorakov, F.N. Pirnazarova, P.G. But, L.A. Piruzyab, V.M. Chibrikin, Y.I. Vikjlyaev, O.V. Ul'yanova, Bull. Acad. Sci. USSR, Div. Chem. Sci. 22 (1973) 2050.
[28] C. Garcia, R. Oyola, L. Piñero, N. Cruz, F. Alejando, R. Arce, I. Nieves, J. Phys. Chem. 106 (2002) 9794.
[29] L.A. Melton, N. Tuqiang, R.A. Caldwell, J. Am. Chem. Soc. 111 (1989) 457.
[30] W. Schnabel, Q. Zhu, P. Jacques, J. Chem. Soc. Faraday Trans. I 87 (1991) 1531.
[31] G.B. Schuster, S.F. Yates, J. Org. Chem. 49 (1984) 3349.
[32] D. Rehm, A. Weller, Isr. J. Chem. 8 (1970) 259.
[33] S. Steenken, L.P. Candeias, J. Am. Chem. Soc. 114 (1992) 699.
[34] U. Lachish, A. Schafferman, G. Stein, J. Phys. Chem. 64 (1976) 4205.
[35] J.W. Hunt, M.J. Bronskill, R.K. Wolff, J. Chem. Phys. 53 (1970) 4201.